1521-0103/12/3422-407–415
THE JOURNAL OF PHARMACOLOGY AND EXPERIMENTAL THERAPEUTICS
U.S. Government work not protected by U.S. copyright
JPET 342:407–415, 2012

Vol. 342, No. 2
191296/3782302

Cerebral Myogenic Reactivity and Blood Flow in Type 2 Diabetic Rats: Role of Peroxynitrite in Hypoxia-Mediated Loss of Myogenic Tone

Aisha I. Kelly-Cobbs, Roshini Prakash, Maha Coucha, Robert A. Knight, Weiguo Li, Safia N. Ogbi, Maribeth Johnson, and Adviye Ergul

Charlie Norwood Veterans Administration Medical Center (W.L., A.E.) and Departments of Physiology (A.I.K.-C., M.C., S.N.O., W.L., A.E.) and Biostatistics (M.J.), Georgia Health Sciences University, Program in Clinical and Experimental Therapeutics, University of Georgia (R.P., A.E.), Augusta, Georgia; and Department of Neurology–NMR Research, Henry Ford Health System, Detroit, Michigan (R.A.K.)

Received December 26, 2011; accepted May 7, 2012

ABSTRACT

Dysregulation of cerebral vascular function and, ultimately, cerebral blood flow (CBF) may contribute to complications such as stroke and cognitive decline in diabetes. We hypothesized that 1) diabetes-mediated neurovascular and myogenic dysfunction impairs CBF and 2) under hypoxic conditions, cerebral vessels from diabetic rats lose myogenic properties because of peroxynitrite ($ONOO^-$)-mediated nitration of vascular smooth muscle (VSM) actin. Functional hyperemia, the ability of blood vessels to dilate upon neuronal stimulation, and myogenic tone of isolated middle cerebral arteries (MCAs) were assessed as indices of neurovascular and myogenic function, respectively, in 10- to 12-week control and type 2 diabetic Goto-Kakizaki rats. In addition, myogenic behavior of MCAs, nitrotyrosine (NY) levels, and VSM actin content were measured under normoxic and hypoxic [oxygen glucose deprivation (OGD)] conditions with and without the $ONOO^-$ decomposition catalyst 5,10,15,20-tetrakis(4-sulfonatophenyl) prophyrinato iron (III), chloride (FeTPPs). The percentage of myogenic tone was higher in diabetes, and forced dilation occurred at higher pressures. Functional hyperemia was impaired. Consistent with these findings, baseline CBF was lower in diabetes. OGD reduced the percentage of myogenic tone in both groups, and FeTPPs restored it only in diabetes. OGD increased VSM NY in both groups, and although FeTPPs restored basal levels, it did not correct the reduced filamentous/globular (F/G) actin ratio. Acute alterations in VSM $ONOO^-$ levels may contribute to hypoxic myogenic dysfunction, but this cannot be solely explained by the decreased F/G actin ratio due to actin nitration, and mechanisms may differ between control and diabetic animals. Our findings also demonstrate that diabetes alters the ability of cerebral vessels to regulate CBF under basal and hypoxic conditions.

Introduction

Type 2 diabetes (T2D) promotes widespread morphological and functional aberrations within the cardiovascular system, including the cerebral vessels (Mayhan, 1993). As a consequence, impairment of intrinsic mechanisms that safeguard the brain against disruptions in blood flow increases the risk of developing microvascular and macrovascular complications, such as acute ischemic stroke (Reusch, 2003; Fowler, 2008) and cognitive decline (Carlsson, 2010; Humpel, 2011). The brain is composed of highly metabolic neural tissue that is completely dependent upon sufficient blood flow for providing nutrients and clearing metabolic wastes (Drake and Iadecola, 2007). The importance of adequate cerebral perfusion is underscored by the fact that, under normal conditions, 1) neural and metabolic cues ensure proper distribution of

This work was supported in part by the National Institutes of Health National Institute of Neurological Disorders and Stroke [Grant F31-NS066746] (to A.I.K.-C.). Additional support was provided in part by a Veteran's Affairs Merit Award [BX000347]; the National Institutes of Health National Institute of Neurological Disorders and Stroke [Grant NS054688]; and an American Heart Association Established Investigator Award [0740002N] (to A.E.). A.E. is a research pharmacologist at the Charlie Norwood Veterans Affairs Medical Center in Augusta, Georgia.

Part of this work was previously presented as follows: Kelly-Cobbs A and Ergul A (2010) Hypoxia reduces cerebrovascular myogenic reactivity in diabetes. *Experimental Biology Conference*; 2010 Apr 25; Anaheim, CA. Federation of American Societies for Experimental Biology, Bethesda, MD. Kelly-Cobbs A, Prakash R, Li W, and Ergul A (2011) Peroxynitrite disrupts cerebrovascular actin cytoskeleton and reduces myogenic reactivity in diabetes after oxygen-glucose deprivation. *International Stroke Conference*; 2011 Feb 10; Los Angeles, CA. American Heart Association, Dallas, TX. Li W, Lima VV, Prakash R, Ogbi S, Tostes R, and Ergul A (2011) Diet-induced obesity impairs neurovascular coupling and increases the damage caused by ischemic stroke; *International Stroke Conference*; 2011 Feb 11, Los Angeles, CA. American Heart Association, Dallas, TX.

Article, publication date, and citation information can be found at http://jpet.aspetjournals.org.

http://dx.doi.org/10.1124/jpet.111.191296.

ABBREVIATIONS: T2D, type 2 diabetes; FeTPPs, 5,10,15,20-tetrakis(4-sulfonatophenyl)prophyrinato iron (III), chloride; CBF, cerebral blood flow; OGD, oxygen glucose deprivation; MCA, middle cerebral artery; PCA, posterior cerebral artery; ROI, region of interest; LD, lumen diameter; MT, media thickness; VSM, vascular smooth muscle; STZ, streptozotocin; GK, Goto-Kakizaki; OD, outer diameter; NO, nitric oxide.

blood flow; 2) autoregulation protects the brain against fluctuations in the systemic circulation (Johnson, 1964); and 3) neuronal activity is tightly coupled to blood flow demand (functional hyperemia) (Iadecola, 2004; Girouard and Iadecola, 2006). Reduced cerebral blood flow (CBF) has been described in diabetic patients as well as in animal models of type 1 diabetes (Duckrow et al., 1987), which may contribute to the progression of neurodegenerative disorders (Iadecola, 2004; Ohara et al., 2011) and complicate ischemia/reperfusion injury in diabetes (Hasselbalch et al., 2001; Li et al., 2010). The basal tension within the cerebral vascular smooth muscle (VSM), termed "myogenic tone," permits dynamic flow changes in response to the energetic demands of the neuronal tissue and is an important modulator of CBF autoregulation (Osol et al., 1991; Cipolla et al., 1997a). In the brain, large arteries such as the middle cerebral arteries (MCAs) contribute 20 to 30% of the total cerebrovascular resistance (Faraci and Heistad, 1990). Zimmermann et al. (1997) demonstrated that MCAs isolated from streptozotocin (STZ)-induced diabetic rats exhibit enhanced constriction. Likewise, Jarajapu et al. (2008) reported altered myogenic reactivity and increased tone in posterior cerebral arteries (PCAs) from type 2 diabetic BBZDR/Wor rats. However, the effect of diabetes on functional hyperemia, myogenic tone, and CBF in a T2D model that mimics blood glucose levels seen in patients remains to be determined.

The autoregulatory efficiency of cerebral vessels is dependent upon polymerization and depolymerization of VSM actin filaments in response to changes in transmural pressure across the vessel (Cipolla and Osol, 1998). The cytoskeletal machinery is particularly vulnerable to oxidative stress (Maneen et al., 2006; Maneen and Cipolla, 2007). Peroxynitrite ($ONOO^-$), a stable reactive oxygen and nitrogen species, is capable of dismantling filamentous (F) actin and preventing globular (G) actin polymerization (Clements et al., 2003; Tiago et al., 2006). Together, these events can lead to an impaired VSM myogenic response (Cipolla et al., 2001; Maneen et al., 2006; Maneen and Cipolla, 2007). Loss of myogenic activity is particularly detrimental during focal cerebral ischemia, where it can contribute to perturbation of vascular integrity and ensuing hemorrhage and edema (Maneen et al., 2006; Dohmen et al., 2007; Maneen and Cipolla, 2007). Previous studies have reported diminished myogenic tone in PCAs isolated from normoglycemic rats after transient middle cerebral artery occlusion (Cipolla et al., 2001; Maneen et al., 2006; Maneen and Cipolla, 2007). Furthermore, this loss of tone was correlated with an $ONOO^-$-mediated decrease in VSM F actin. Because of the potential mechanical injury sustained from transient middle cerebral artery occlusion beyond 30 min (Cipolla et al., 2001); however, there are few studies examining the effects of ischemia/reperfusion injury on MCA myogenic reactivity. Furthermore, the mechanisms underlying the impairment of myogenic reactivity observed in diabetes, particularly under hypoxic conditions, are not fully understood. Thus, the purpose of our study was to use an ex vivo oxygen glucose deprivation (OGD) protocol that would enable us to test the hypothesis that basal cerebrovascular myogenic tone is increased in the Goto-Kakizaki (GK) rat model of T2D diabetes and that after OGD, cerebral vessels from these chronically diabetic rats will have markedly reduced myogenic reactivity due to $ONOO^-$-mediated nitration of the VSM actin cytoskeleton.

Materials and Methods

Animals. All experiments were performed on 10- to 12-week-old male Wistar rats ($n = 31$) (Harlan, Indianapolis, IN) and age-matched diabetic GK rats ($n = 33$) (in-house bred, derived from the Tampa colony). This age range was based on our previous studies that showed greater vascular injury, hemorrhage, and edema in this model at this age after ischemia/reperfusion injury of the brain. Glucose intolerance can be observed as early as 2 weeks of age in the GK rat, and onset of moderate hyperglycemia can be as early as 5 to 6 weeks of age. During weeks 6 to 12, plasma insulin levels are elevated and then decrease to levels lower than that observed in Wistar rats (Goto et al., 1976; Harris et al., 2005). This nonobese model of T2D is ideal for these studies because diabetes-induced cerebrovascular alterations can be studied in the absence of confounding comorbidities such as hypertension or hyperlipidemia (Harris et al., 2005; Elgebaly et al., 2008). The animals were housed at the Georgia Health Sciences University animal care facility, which is approved by the American Association for Accreditation of Laboratory Animal Care. All protocols were approved by the institutional animal care and use committee. Animals were fed standard rat chow and tap water ad libitum. Body weights and blood glucose measurements were taken biweekly. Blood glucose measurements were taken from tail vein samples using a commercially available glucometer (Freestyle; Abbott Diabetes Care, Inc., Alameda, CA). Mean arterial pressure (millimeters mercury) was measured using the tail-cuff method. All animals were anesthetized with pentobarbital sodium (Fatal-Plus; Vortech Pharmaceuticals Ltd., Dearborn, MI), exsanguinated via cardiac puncture, and decapitated to extract the brain.

Measurement of Functional Hyperemia. Functional hyperemia was assessed 2 days before ischemic injury by measuring the changes in CBF in the somatosensory cortex upon whisker stimulation. For this purpose, trimmed contralateral whiskers were gently stroked at a frequency of 2.5 Hz using a cotton tip attached to a vortex (Kaarisalo et al., 2005; Nicolakakis et al., 2008). A PIM 3 laser Doppler flow meter (Perimed Systems, Stockholm, Sweden) was programmed to scan an area covering somatosensory cortex, which is supplied by the MCA. Changes in CBF were expressed as percentage increase relative to resting levels. The laser beam was directed at the skull surface (2-mm posterior and 5-mm lateral to bregma) by a moving-mirror system in the scanner without tissue contact. In this system, a built-in photo detector identifies the reflected light from moving blood cells within 0.5 cm of the cortical surface, and a color-coded image is acquired based on the concentration and mean velocity of these blood cells using the LDPIwin software (Perimed, North Royalton, OH).

Measurement of CBF by Magnetic Resonance Imaging. All magnetic resonance imaging measurements of CBF were acquired using a 7-tesla, 20-cm bore magnet interfaced to a Bruker console. The animals were initially anesthetized using 1.0 to 2.0% isoflurane in a 2:1 N_2O/O_2 gas mixture administered by spontaneous respiration. After induction, the animals were placed on a plastic platform equipped with ear bars to stabilize the head and a nose cone for administration of gases. The platform then fits inside a 5-cm-diameter quadrature transmit/receive birdcage coil tuned to the resonant frequency of water (300 MHz). CBF measures were obtained in cerebral tissue using an arterial spin-labeling technique (Detre et al., 1992; Williams et al., 1992). Adiabatic inversion of inflowing arterial water proton (Dixon et al., 1986) was accomplished via an axial gradient of ± 0.3 kHz/mm and a 1-s continuous-wave radiofrequency power of approximately 0.3 kHz at a frequency offset of ± 6 kHz. This was followed by a spin-echo imaging sequence with a repetition time/echo time of 1000 ms/20 ms. As indicated, four preparations of the image were acquired with the gradient polarities and frequency

offsets switched to remove the gradient asymmetry in the axial direction. The labeled slice is 2-cm distal from the imaging slice with 1-mm thickness. The field of view was 32 × 32 mm with a 64 ′ 64 matrix size. Whereas this study did not use MCA occlusion to induce ischemia, the regions of interest (ROI) for CBF measurements were based on regions where brain infarcts occur if the MCA is occluded and included entire parietal cortex or striatum (Knight et al., 1998).

MCA Function and Morphometry. MCAs were quickly excised and used within 45 min of isolation to ensure viability of the vessels. A pressure arteriograph system (Living Systems, Burlington, VT) was used to evaluate MCA structure, myogenic tone, and mechanical properties. For these studies, MCA segments approximately 200 to 250 μm in diameter and proximal to the junction between the MCA and the inferior cerebral vein were used exclusively. The vessels were first mounted onto glass cannulas in an arteriograph chamber, and HEPES bicarbonate buffer (130 mM NaCl, 4 mM KCl, 1.2 mM $MgSO_4$, 4 mM $NaHCO_3$, 10 mM HEPES, 1.18 mM KH_2PO_4, 5.5 mM glucose, and 1.8 mM $CaCl_2$) was circulated and maintained at 37 ± 0.5°C. The MCA segments were then pressurized at 20 mm Hg for 1 h to generate spontaneous tone. A video dimension analyzer connected to the arteriograph system was used to measure media thickness (MT) and lumen diameter (LD) at pressures ranging from 0 to 180 mm Hg, in 20-mm Hg increments. The first measurement was taken at 5 mm Hg because negative pressure is generated at 0 mm Hg, causing the vessel to collapse. All vessels were exposed to each pressure point for 5 min before readings were recorded. Pressure-diameter curves were obtained first in the presence of Ca^{2+} to observe the vessels' contractile properties and then in Ca^{2+}-free buffer with the addition of 10^{-7} M papaverine hydrochloride to evaluate the vessels' passive properties.

Data Calculations. Using the MT and LD measurements obtained in active conditions (in the presence of Ca^{2+}) and in passive conditions (in the absence of Ca^{2+}), the following parameters related to MCA structure, myogenic tone, and mechanical properties can be calculated: MT (micrometer) = left wall + right wall; outer diameter (OD; micrometer) = LD + MT; medial/lumen ratio (M/liter) = MT/LD; and percentage myogenic tone (percentage tone) = 1 − (active OD/passive OD) × 100.

Ex Vivo Oxygen-Glucose Deprivation. A modified ex vivo OGD protocol (Lynch et al., 2006) was used to determine the effects of OGD on MCA structure, myogenic tone, and mechanical properties. Pressurized MCA segments approximately 250 μm in diameter were first equilibrated at 20 mm Hg for 1 h in HEPES buffer containing 5.5 mM glucose to allow the development of spontaneous tone. Immediately after the equilibration period, induction of OGD was performed by sealing off the arteriograph chamber and connecting it to a gas line supplying 95% N_2/5% CO_2 at a rate of 20 ml/min while low glucose (1 mM) HEPES buffer, also gassed with the N_2/CO_2 mixture, was circulated and maintained at 37 ± 0.5°C. The MCAs were exposed to OGD for 20 min before they were returned to normoxic conditions, and buffer containing 5.5 mM glucose was recirculated for the remainder of the experiment. Pressure-diameter curves were obtained as described above.

Acute Treatment with FeTPPs or Peroxynitrite. To determine the effects of acute antioxidant treatment on vascular structure and function, vessels were equilibrated for 1 h and subjected to 20 min of OGD exposure as described in the previous section, and the peroxynitrite decomposition catalyst 5,10,15,20-tetrakis(4-sulfonatophenyl) prophyrinato iron (III), chloride (FeTPPs; 2.5 μM) (Sharma et al., 2007; Abdelsaid et al., 2010) (Calbiochem, San Diego, CA) was added to the recirculating HEPES buffer immediately after OGD treatment and allowed to circulate for the remainder of the experiment. To further investigate the effect of peroxynitrite on control and diabetic vessels, MCAs isolated from right and left side of the same animal were treated with either vehicle or peroxynitrite (10 μM) in the arteriograph chamber after the equilibration period and then pressure curves were obtained.

Detection of Hypoxia. To confirm hypoxia ($pO_2 < 10$ mm Hg) in MCAs exposed to OGD, whole MCA segments were treated with 200 μM pimonidazole hydrochloride (Natural Pharmacia International, Inc., Burlington, MA). The MCA segments were first equilibrated at 20 mm Hg for 1 h and then pressure fixed in 4% paraformaldehyde in PBS after OGD exposure. A Hypoxyprobe-1 Omni kit (catalog number HPI-100); NPI) was used to probe for pimonidazole hydrochloride adducts using conventional immunohistochemical methods. Images of stained vessels (40×, oil) were captured using an inverted confocal microscope (LSM 510; Carl Zeiss Inc., Thornwood, NY) and processed using Zen 2008 software.

F and G Actin Staining and Quantification. The MCA segments were pressure fixed in methanol-free 4% paraformaldehyde in PBS for 1 h at 20 mm Hg. Whole-mounted tissues were then stained with Oregon Green 488-conjugated phalloidin fluorescent probe (Invitrogen, Carlsbad, CA) and Alexa 594-conjugated DNase I (Invitrogen) to identify F and G actin cytoskeletal proteins, respectively. Stained vessels were opened lengthwise by a longitudinal cut with microsurgical scissors (Fine Science Tools, Foster City, CA) and mounted for imaging. *Z*-stacks (8 μm; 0.5 μm intervals) of the VSM layer were captured at 63× using an LSM 510 inverted confocal microscope and processed using Zen 2008 software. This ROI was confirmed by staining for nuclei in a separate set of vessels and observing their distinctive parallel arrangement. ImageJ software (National Institutes of Health, Bethesda, MD) was used to quantify F and G actin volume intensity.

Nitrotyrosine Quantification. Nitrotyrosine levels were used as an indirect marker of $ONOO^-$ generation in blood plasma and MCAs. Snap-frozen MCAs were homogenized as described previously (Harris et al., 2005; Portik-Dobos et al., 2006; Elgebaly et al., 2007). Total nitrotyrosine levels were determined via slot blot analysis using an anti-nitrotyrosine monoclonal antibody (Millipore Corporation, Billerica, MA).

Statistical Analysis. Data are expressed as mean ± S.E. Data were evaluated for normality, and appropriate transformations were used when necessary. A rank transformation was used for MCA nitrotyrosine levels before analysis. Area under the curve across intraluminal pressure (60–160 mm Hg) was calculated using NCSS 2007 (NCSS, LLC, Kaysville, UT). A series of analyses were used to assess the effect of disease and treatment. A 2 disease (control vs. diabetes) by 2 OGD (no vs. yes) analysis of variance was used to assess the effect of hypoxia on diseased vessels. A 2 disease + OGD (control vs. diabetes) × 2 FeTPPs (no vs. yes) analysis of variance was used to assess the effect of FeTPPs treatment on disease vessels after OGD exposure. An interaction would indicate a differential effect of hypoxia or FeTPPs treatment on diabetic vessels. A Tukey's test was used to adjust for the multiple comparisons used to assess significant effects. Statistical significance was determined at $\alpha = 0.05$. SAS version 9.2 (SAS Institute, Cary, NC) was used for all analyses.

Results

Metabolic Parameters. Metabolic parameters for experimental groups are summarized in Table 1. GK rats are a lean model of T2D. These spontaneously diabetic animals were smaller than their age-matched controls and, beginning

TABLE 1
Metabolic parameters of experimental animals
Results are given as mean ± S.E.

Metabolic Parameters	Control (n = 31)	Diabetes (n = 33)
Weight, g	310 ± 2.6	296 ± 4.8*
Glucose, mg/dl	97.5 ± 2.3	180.0 ± 8.2†††
Mean arterial pressure, mm Hg	102 ± 1	108 ± 5

* $p < 0.05$ vs. control.
††† $p < 0.001$ vs. control.

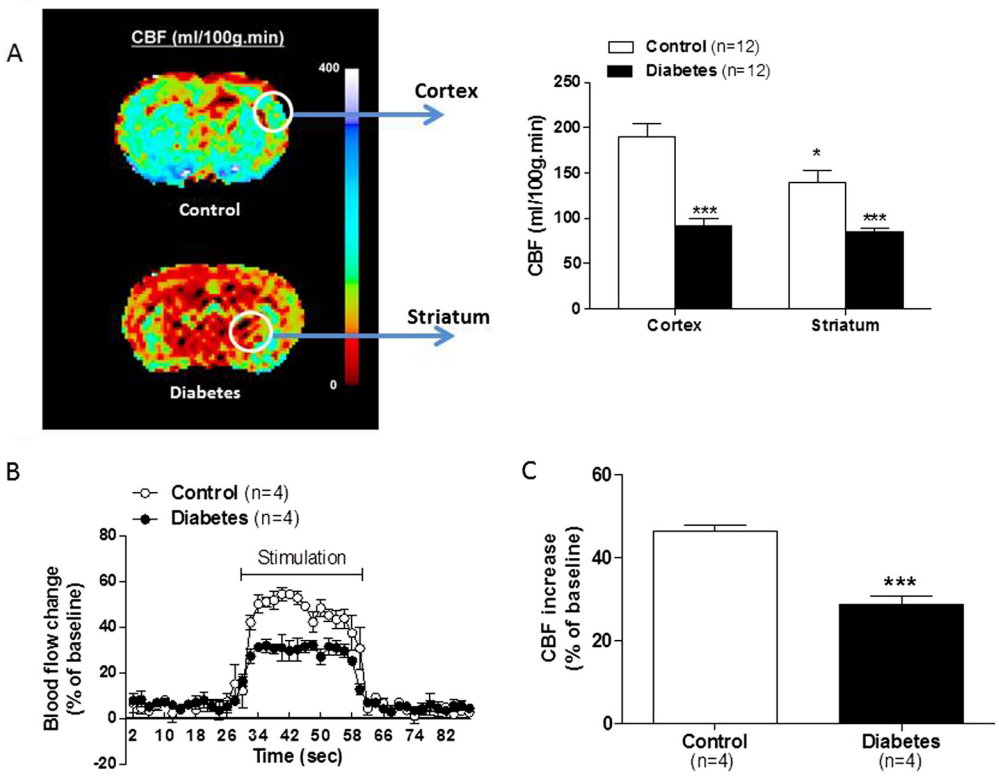

Fig. 1. CBF and functional hyperemia are compromised in diabetes. A, a representative color-coded image of CBF obtained by magnetic resonance imaging is shown on the left. Quantitative analysis of readings in the parietal cortex or striatum (indicated by white circles) from all animals is given in the bar graphs on the right. B, tracing of changes in CBF as measured by laser Doppler directed at 2-mm posterior and 5-mm lateral to bregma scanning during whisker stimulation in anesthetized animals. C, average of the percentage CBF change given in B over the stimulation period. Results are given as mean ± S.E.; $n = 4–12$. *, $p < 0.05$ vs. cortex; ***, $p < 0.001$ vs. control.

at 6 weeks of age, displayed moderate hyperglycemia, as reported previously (Harris et al., 2005; Elgebaly et al., 2008). Blood pressure was slightly higher in diabetic animals compared with controls; however, these animals were not hypertensive.

CBF and Functional Hyperemia. Basal CBF measurements yielded two important findings. First, CBF in parietal/insular cortex and striatum was significantly lower in diabetic animals compared with controls (Fig. 1A). Second, cortical CBF was greater than that measured in the striatum of control animals, but this difference was not observed in diabetic animals. In addition, relative increases in CBF upon stimulation of somatosensory cortex were lower in diabetic animals, indicating impaired functional hyperemia and neurovascular coupling (Fig. 1, B and C).

MCA Myogenic Tone and Reactivity. Increasing intraluminal pressures from 80 to 180 mm Hg generated greater myogenic tone in isolated MCAs from chronically diabetic rats, compared with their age-matched controls (Fig. 2A). Short-term OGD exposure diminished MCA myogenic response to increases in pressure from 20 to 180 mm Hg (Fig. 2B). This reduced myogenic reactivity is particularly evident in MCAs from diabetic rats. The addition of FeTPPs after OGD treatment restored basal myogenic tone in vessels from diabetic rats, whereas control vessels were not affected (Fig. 2C).

Active pressure-diameter curves indicate that MCAs from diabetic rats constrict more in response to increases in pressure and forced dilatation occurs at higher pressures (Fig. 2D). Active LDs were increased in all MCAs exposed to ex vivo OGD; however, they were still capable of generating a blunted autoregulatory response (Fig. 2E). Acute FeTPPs treatment did reverse the effects of OGD on active LDs in the diabetic group but not in the control group (Fig. 2F). To further confirm that peroxynitrite impacts myogenic reactivity and tone to a greater extent in diabetes, MCAs isolated from control or diabetic animals were treated with vehicle or peroxynitrite under normoxic conditions. Although the myogenic tone of MCAs from control animals did not change in the presence of peroxynitrite, vessels from diabetic animals displayed a 39.4 ± 1.6 and 69.3 ± 16.9% loss in myogenic tone at 100- and 140 mm-Hg pressures, respectively, supporting our hypothesis that cerebral vessels are highly sensitive to peroxynitrite in diabetes.

Confocal imaging results confirmed that hypoxia was detected only in MCAs incubated in pimonidazole hydrochloride at the time of OGD exposure. The presence of pimonidazole hydrochloride or OGD alone was not sufficient to detect hypoxia in these vessels (Fig. 2, inset).

MCA Structure. After 6 weeks of moderate hyperglycemia exposure, MCA MT is indistinguishable from control vessels (Fig. 3A). Arteriograph results also indicated MT was increased in all vessels exposed to OGD (Fig. 3B). OGD-mediated media thickening was not reversed in control vessels after FeTPPs treatment (Fig. 3C).

Passive dilatation obtained under calcium-free conditions was similar to normoglycemic controls over the entire range of intraluminal pressures (Fig. 3D). Passive LDs did not change after OGD treatment (Fig. 3E) or after peroxynitrite scavenging with FeTPPs (Fig. 3F).

Media-to-lumen ratios observed in MCAs from diabetic rats were similar to those of control vessels at all pressure points (Fig. 3G). At pressures beyond 40 mm Hg, OGD exposure resulted in higher media-to-lumen ratios in both control and diabetic vessels (Fig. 3H). FeTPPs treatment had no effect on the media-to-lumen ratios from either OGD-treated group (Fig. 3I).

F and G Actin Quantification. Using confocal imaging, the VSM layer was identified by its distinctive parallel

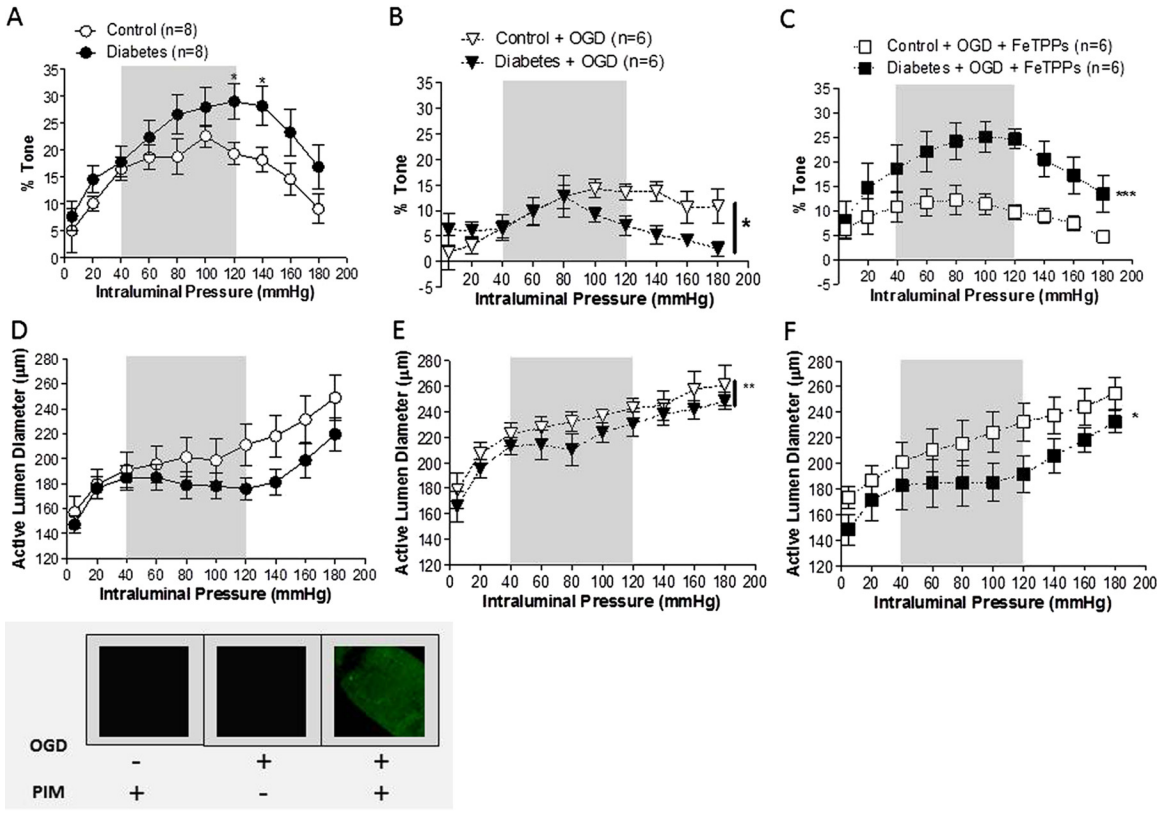

Fig. 2. Effects of diabetes, OGD, and acute antioxidant treatment on myogenic responses in isolated MCAs over increasing intraluminal pressures. A, myogenic tone at intraluminal pressures of 120 and 140 mm Hg was increased in MCAs after 6 weeks of diabetes exposure. *, $p < 0.05$ vs. control. B, a 2 (control vs. diabetes) × 2 (untreated vs. OGD) analysis of data shown here and in A indicated that the OGD reduced tone, and this was greater in diabetes. *, $p < 0.05$ vs. untreated or control + OGD. C, a 2 (untreated vs. OGD) × 2 (vehicle vs. FeTPPS) analysis of data shown here and in B indicated that FeTPPs (2.5 μM) reversed OGD-induced reduction in tone only in vessels from diabetic animals. ***, $p < 0.001$ vs. OGD. D, although not significant, the MCAs from chronically diabetic rats demonstrated a rightward shift in the autoregulatory curve. E and F, furthermore, OGD increased the active LDs of MCAs (E) and acute antioxidant treatment with FeTPPs after OGD exposure restored basal levels only in diabetic animals (F). *, $p < 0.05$ vs. OGD. **, $p < 0.01$ (untreated vs. OGD). Inset, the presence of hypoxia during OGD exposure was confirmed with pimonidazole hydrochloride. Gray areas denote the normal autoregulatory range (40–120 mm Hg) for MCAs. PIM, pimonidazole hydrochloride. Results are given as mean ± S.E.; $n = 6–8$.

arrangement of cells, and Z-stacks of this ROI were captured and processed (Fig. 4A). In untreated vessels, F/G actin ratios were similar. Furthermore, OGD exposure irreversibly reduced F/G ratios in both control and diabetic vessels. FeTPPs treatment did not have any effect in either group (Fig. 4B). Nitrotyrosine staining was more pronounced in both control and diabetic vessels after OGD exposure, and this was reduced by FeTPPS treatment (Fig. 4C). In these samples, there was colocalization of G actin and nitrotyrosine staining, suggesting that nitration contributes to the increases in the G actin pool.

MCA Peroxynitrite Generation. Nitrotyrosine quantification was used as an indirect measurement of basal $ONOO^-$ generation in plasma and isolated MCAs from control and diabetic animals. After 6 weeks of diabetes, nitrotyrosine levels in plasma (Fig. 5A) and untreated whole-vessel homogenates (Fig. 5B) were double that of controls. Nitrotyrosine levels were elevated in whole MCA homogenates from OGD-treated control vessels, whereas OGD exposure did not raise nitrotyrosine levels beyond baseline values that are already high in MCAs from diabetic rats. Likewise, acute treatment with FeTPPS restored basal nitrotyrosine levels in OGD-treated control vessels, but no significant difference was detected in MCAs obtained from diabetic animals.

Discussion

The objective of the current study was to address the following questions: 1) What structural and functional changes occur in cerebral vessels as a result of chronic diabetes exposure, and how do they affect CBF?; 2) Do cerebral vessels from control and diabetic animals respond similarly to acute OGD?; and 3) Are the effects of OGD mediated by peroxynitrite? Our results indicate that chronic diabetes exposure results in dysregulation of CBF that is accompanied by heightened myogenic reactivity and impaired neurovascular coupling. In the early stages of diabetes, however, pathological structural changes are not present in large cerebral vessels. Short-term OGD blunts cerebrovascular autoregulation and attenuates myogenic responses, irrespective of glycemic status. The loss of myogenic reactivity and tone observed in vessels from diabetic rats is associated with peroxynitrite generation during OGD; however, these effects cannot be solely explained by peroxynitrite-mediated nitration of the VSM actin cytoskeletal filaments.

The brain relies completely upon continuous perfusion by cerebral vessels to ensure the normal health and function of nervous tissue; consequently, the cerebrovasculature is equipped to protect against dramatic fluctuations in blood

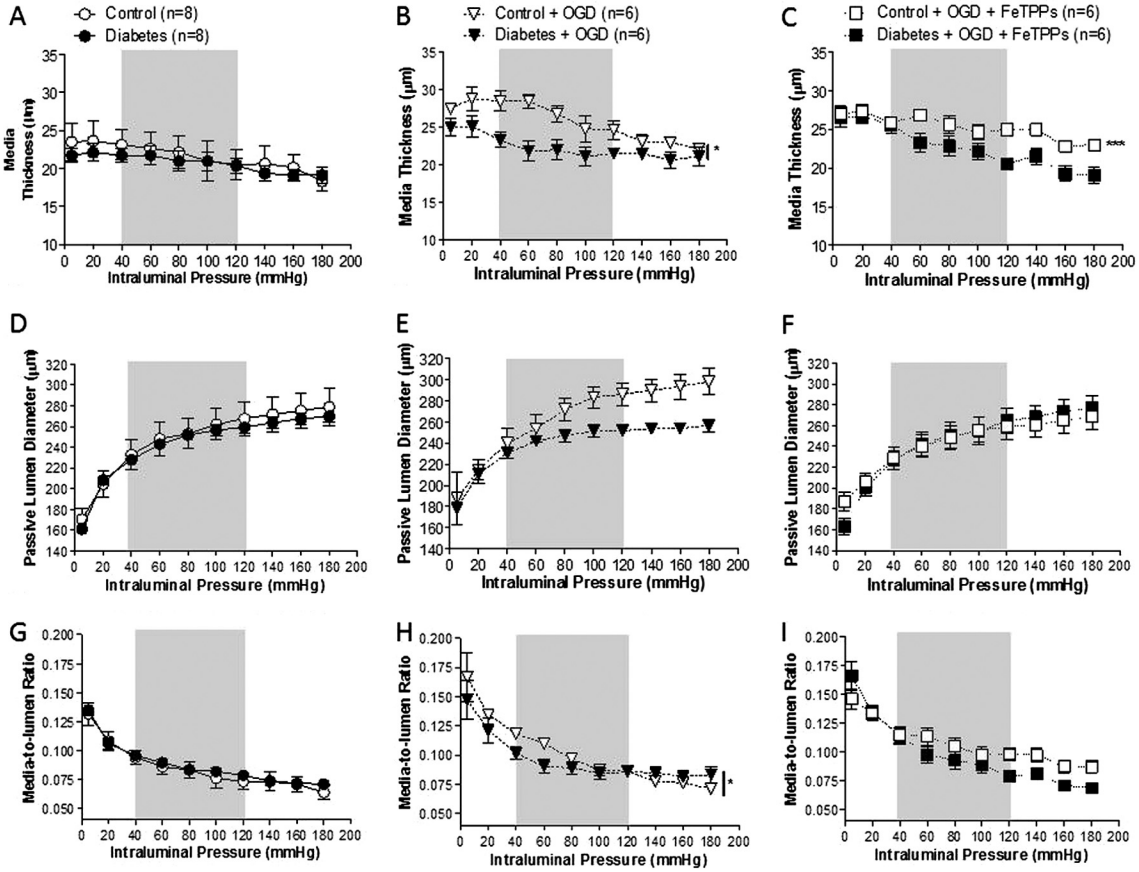

Fig. 3. Effects of diabetes, OGD, and acute antioxidant treatment on MCA structure. A, the MCA MT in early diabetes is similar to untreated control vessels. B, a 2 (control vs. diabetes) × 2 (untreated vs. OGD) analysis of data shown in A and B indicated that the exposure to OGD induced media thickening in MCAs in both groups. *, $p < 0.05$ vs. untreated. C, peroxynitrite scavenging does not correct media thickening in OGD-treated control vessels. ***, $p < 0.001$ vs. OGD. D, under calcium-free conditions, MCA LDs were similar between untreated control and diabetic rats. E and F, there was no change in passive LDs of either control or diabetic MCAs after OGD exposure with (E) or without (F) FeTPPs (2.5 μM). G, media-to-lumen ratios were similar in vessels from untreated control and diabetic rats. H, higher media-to-lumen ratios were observed after OGD exposure. *, $p < 0.05$ vs. untreated. I, FeTPPs had no effect on larger media-to-lumen ratios across the entire range of pressures in OGD-exposed MCAs. Gray areas denote the normal autoregulatory range (40–120 mm Hg) for MCAs. Results are given as mean ± S.E.; $n = 6–8$.

flow. Dysregulation of blood flow and impairment of the regulatory mechanisms that ensure perfusion matches neuronal demand both contribute to the microvascular and macrovascular complications observed in diabetes. In this study, we provide two lines of evidence: 1) functional hyperemia is impaired in diabetes, and 2) basal CBF is reduced in diabetic animals compared with controls. The neurovascular dysfunction observed in the current study may be of vascular or neuronal origin, or both. It is believed that under physiological conditions, functional hyperemia is principally regulated by penetrating parenchymal arterioles, astrocytes, and interneurons (Lecrux and Hamel, 2011). Although penetration of the brain is limited by laser Doppler imaging, whisker stimulation tests allow us to evaluate functional hyperemia by detecting changes in CBF on the surface of the brain. These upstream cortical vessels are innervated by the peripheral nervous system but are also retrogradely affected by changes that occur in deep penetrating arterioles. There is also evidence that oxidative stress contributes to impaired functional hyperemia in other disease models (Girouard and Iadecola, 2006). In our model of T2D, we believe that oxidative stress may also be involved and additional experiments are needed to directly address this possibility. The latter set of data is in accordance with previous reports that chronic diabetes exposure with uncontrolled moderate hyperglycemia contributes to reduced CBF (Duckrow et al., 1987; Kaplar et al., 2009). There are experimental studies that have shown increased CBF in diabetes, but these have primarily been described in acute STZ-induced models of diabetes exhibiting serve hyperglycemia with plasma glucose levels greater than 300 mg/dl (Al-Saeedi, 2008). Finally, failure to detect differences in basal CBF or reports of higher CBF in diabetic patients likely results from a study population with good glycemic control (Neil et al., 1987).

Findings from functional studies regarding the effects of hyperglycemia on cerebrovascular reactivity and tone are also conflicted, stemming from differences in the derivation, duration, and severity of high glucose exposure. Cipolla et al. (1997b) reported that endothelium-dependent nitric oxide (NO) and prostaglandin mechanisms contributed to reduced myogenic tone in PCAs isolated from normoglycemic rats in response to acute exposure to high glucose concentrations; however, these vessels were acutely perfused with physiological buffers containing substantially high glucose levels upward of 790 mg/dl. In this study, we give evidence that despite the absence of pathological remodeling, chronic moderate hyperglycemia contributes to increased myogenic tone and forced dilation at higher pressures in cerebral arteries

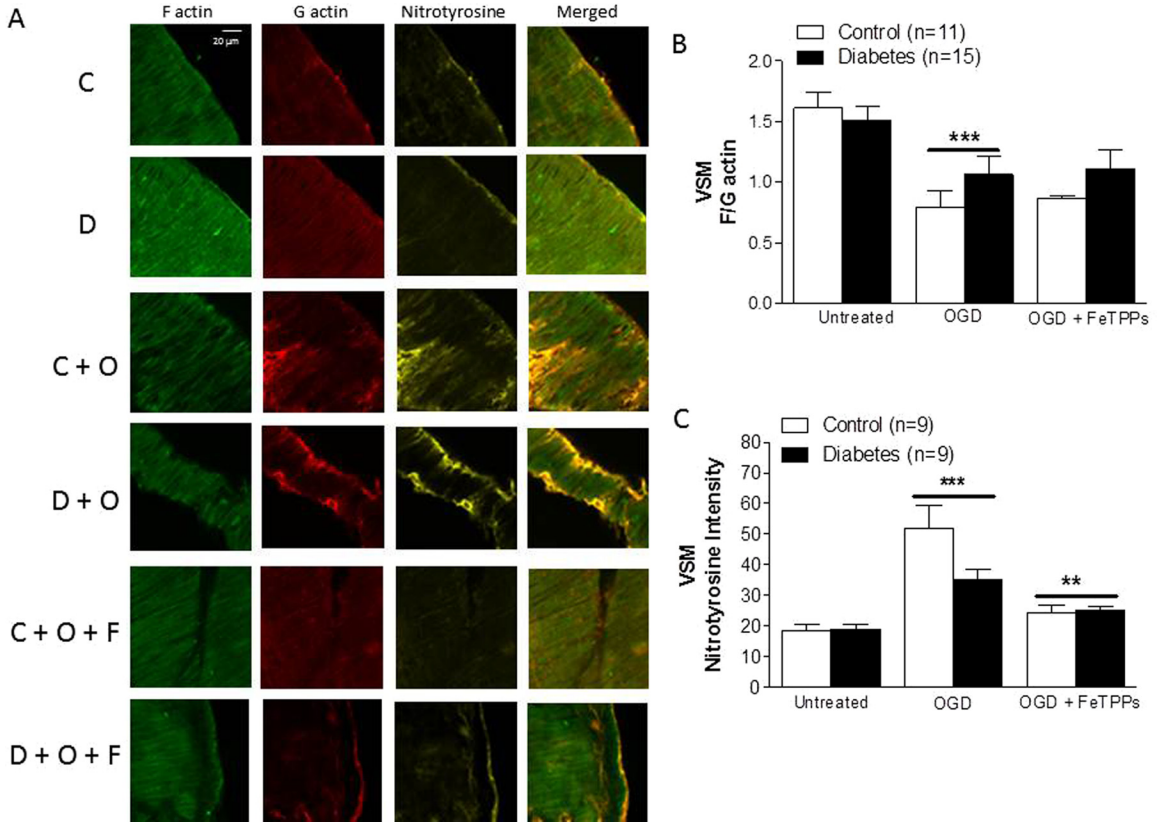

Fig. 4. Effects of diabetes and hypoxia on VSM actin cytoskeleton and total protein nitration. A, representative confocal microscopy images of MCA segments stained for F and G actin cytoskeletal filaments and colocalization of actin filaments with nitrotyrosine. C, control; D, diabetes; C + O, control plus OGD; D + O, diabetes plus OGD; C + O + F, control plus OGD plus FeTPPs; D + O + F, diabetes plus OGD plus FeTPPs. B, a 2 (control vs. diabetes) × 2 (untreated vs. OGD) analysis of data shown indicated that OGD mediated a decrease in the F/G actin ratio in both groups. ***, $p < 0.001$ vs. untreated. FeTPPs (2.5 μM) did not restore the F/G actin ratio in either group. C, VSM nitrotyrosine levels are similar in untreated groups. OGD increased VSM nitrotyrosine levels in MCAs in both groups. ***, $p < 0.001$ vs. untreated. Acute treatment with FeTPPs after OGD exposure reversed this effect. **, $p < 0.05$ vs. OGD. Results are given as mean ± S.E.; $n = 3–4$.

such as the MCA. These data are in agreement with previous observations that vasomotor dysfunction in diabetes precedes the advent of structural pathologies (Bagi et al., 2004; Oizumi et al., 2006). We also reported that metformin treatment started at the onset of diabetes prevents increased myogenic tone in this model, suggesting that hyperglycemia mediates this effect (Elgebaly et al., 2010). Diabetic BBZDR/Wor rats used in the study by Jarajapu et al. (2008) had glucose levels in excess of 400 mg/dl; however, PCAs isolated from in these animals exhibited increased tone after 4 weeks of diabetes resulting from increased phospholipase C activation. These vessels also displayed heightened vascular resistance as evidenced by forced dilation at higher pressures. Likewise, chronic studies by Zimmermann et al. (1997) demonstrated that MCAs isolated from STZ-induced diabetic rats exhibit enhanced constriction and myogenic tone attributed to hyperglycemia-mediated increases in membrane depolarization because of diminished responses to ATP-sensitive potassium-channel openers.

As the incidence of T2D rises worldwide, there is an increasingly urgent need for effective therapies targeted to this stroke-prone population. However, it is not fully understood how diabetes-mediated changes in the cerebrovasculature contribute to ischemia-reperfusion injury. Our ex vivo OGD studies were conducted to see whether we would observe similar results from previous functional studies reported in cerebral vessels exposed to ischemia/reperfusion injury in normoglycemic animals that had undergone transient focal cerebral ischemia (Cipolla et al., 2001; Cipolla and Curry, 2002; Maneen et al., 2006; Maneen and Cipolla, 2007; Jime-

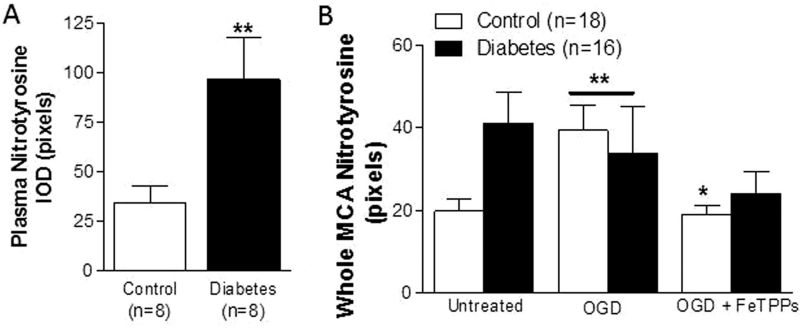

Fig. 5. Effect of diabetes on circulating and tissue (MCA) nitrotyrosine levels. A, basal nitrotyrosine (NY) levels are higher in plasma samples from chronically diabetic rats. **, $p < 0.01$ vs. control. B, a 2 (control vs. diabetes) × 2 (untreated vs. OGD) analysis of data indicated that there is a disease and treatment interaction in response to OGD treatment in control vs. diabetic vessels. OGD increases whole MCA nitrotyrosine levels in control but not in diabetes. **, $p < 0.01$ vs. untreated. Treatment with FeTPPs (2.5 μM) counteracts this response in controls without any effect on diabetic vessels. *, $p < 0.05$ vs. OGD. IOD, integrated optical density. Results are given as mean ± S.E.; $n = 3–8$.

nez-Altayo et al., 2009; Perez-Asensio et al., 2010). In particular, we were curious to see whether OGD-treated vessels isolated from moderately hyperglycemic rats would also exhibit loss of tone due to decreases in VSM F/G actin ratios and increases in LD and wall thickness. Consistent with aforementioned studies, we provide evidence that vessels from control animals display reduced tone associated with reduced F/G actin ratios. We also observed the protective hypertrophy and vasodilator responses that reduce wall stress in response to hypoxia (Jimenez-Altayo et al., 2009). Myogenic tone was also dramatically reduced in MCAs from diabetic animals, and this was associated with decreased F/G actin ratio and increased MT.

Alone, hyperglycemia increases both superoxide (O_2^-) and NO levels, driving the production of the cytotoxic radical $ONOO^-$ while reducing NO bioavailability within the vasculature (El-Remessy et al., 2010); however, $ONOO^-$ is also generated during ischemia/reperfusion (Fukuyama et al., 1998; Gursoy-Ozdemir et al., 2004). Peroxynitrite is capable of thiol oxidation and tyrosine nitration, both of which can alter the function of enzymes and other cellular components (Fukuyama et al., 1998; Turko and Murad, 2002). Our present findings suggest that type 2 diabetic GK rats have greater plasma nitrotyrosine levels compared with normoglycemic controls, consistent with data published in humans (Turko and Murad, 2002). Furthermore, nitrotyrosine levels in whole MCA homogenates isolated from diabetic rats were double that of controls. In light of our functional data, we predicted that nitrotyrosine levels in MCAs exposed to ex vivo OGD/reperfusion would be higher than isolated control vessels exposed to the same intervention. Furthermore, we anticipated that acute antioxidant treatment with FeTPPs would result in a greater reduction in the vessels isolated from diabetic animals. However, the data obtained show that nitrotyrosine levels are greater in whole MCAs from control and diabetic rats after OGD and FeTPPs reduces nitrotyrosine in both groups. When we examined the nitrotyrosine levels within the VSM of untreated MCAs using confocal microscopy, we found that levels were similar in control and diabetic rats at baseline and after OGD. On the basis of these findings, we can deduce that in early diabetes, the endothelium is the primary contributor of peroxynitrite generation and may impact potassium channels and endothelial nitric oxide synthase activity. There is evidence to suggest that calcium-activated endothelial potassium channels influence myogenic tone (Zimmermann et al., 1997) and any alterations in the activity of these targets may contribute to the greater cerebrovascular myogenic tone we observe in diabetic animals. Finally, previous studies have reported that reductions in myogenic tone after ischemic injury in otherwise healthy animals were associated with increased $ONOO^-$ and nitrotyrosine formation that colocalized with actin (Maneen et al., 2006; Maneen and Cipolla, 2007). Our current study provides evidence that diminished myogenic tone in isolated vessels cannot be solely explained by tyrosine nitration of F actin since $ONOO^-$ scavenging prevented nitrotyrosine formation but did not restore F/G actin ratios in control vessels. FeTPPs did not restore myogenic tone, either. These findings suggest that in control vessels, another mechanism may be contributing to the decrease in F/G actin ratio and accompanying loss of tone. In diabetes, however, FeTPPs does not prevent the decrease in F/G actin ratio but is able to restore tone implicating that there must be other targets of $ONOO^-$ that contribute to the regulation of tone in diabetes, such as large calcium-activated potassium channels (BK channels) on VSMCs. Alternatively, $ONOO^-$ might modify the actin cytoskeleton by another mechanism such as thiol oxidation.

There are several limitations to this study. Whereas hypoxia was detected in the ex vivo preparation, we have not been able to determine whether the levels of hypoxia replicate those observed in ischemia/reperfusion injury in vivo. Second, based on previous studies, we postulated that the effects observed in OGD would be mediated by $ONOO^-$; however, we cannot discount the contribution of other sources of oxidative and nitrosative stress on vascular reactivity, tone, and structure. Also, it is possible that the irreversible reduction in actin cytoskeleton polymerization observed in OGD-treated vessels results in oxidative stress-mediated glutathionylation of actin cysteinyl residues or protein aggregation due to carbonylation and may not be the result of protein nitration, as previous hypothesized (Johansson and Lundberg, 2007; Dailianis et al., 2009). Finally, the results obtained in vessels from diabetic animals cannot be explained solely by the effects of oxidative stress generated during hypoxic conditions. Hyperglycemia also promotes abnormal responses to vasoactive agents (Schwaninger et al., 2003; Didion et al., 2005). For example, we have reported that MCAs and BAs from type 2 diabetic rats have heightened sensitivity to the vasoconstrictor endothelin-1 that is abolished by chronic endothelin receptor blockade (Harris et al., 2008). Thus, cerebral dysfunction in diabetes is multifactorial in nature, and by uncovering these mechanisms, we can implement better strategies to safeguard against vascular complications of the disease.

Authorship Contributions

Participated in research design: Kelly-Cobbs, Knight, and Ergul.

Conducted experiments: Kelly-Cobbs, Prakash, Coucha, Knight, Li, and Ogbi.

Performed data analysis: Kelly-Cobbs, Knight, Li, Johnson, and Ergul.

Wrote or contributed to the writing of the manuscript: Kelly-Cobbs, Prakash, Knight, Li, Johnson, and Ergul.

References

Abdelsaid MA, Pillai BA, Matragoon S, Prakash R, Al-Shabrawey M, and El-Remessy AB (2010) Early intervention of tyrosine nitration prevents vasoobliteration and neovascularization in ischemic retinopathy. *J Pharmacol Exp Ther* **332:**125–134.

Al-Saeedi FJ (2008) Perfusion scanning using 99mTc-HMPAO detects early cerebrovascular changes in the diabetic rat. *BMC Med Phys* **8:**1.

Bagi Z, Toth E, Koller A, and Kaley G (2004) Microvascular dysfunction after transient high glucose is caused by superoxide-dependent reduction in the bioavailability of NO and BH(4). *Am J Physiol Heart Circ Physiol* **287:**H626–H633.

Carlsson CM (2010) Type 2 diabetes mellitus, dyslipidemia, and Alzheimer's disease. *J Alzheimers Dis* **20:**711–722.

Cipolla MJ and Curry AB (2002) Middle cerebral artery function after stroke: the threshold duration of reperfusion for myogenic activity. *Stroke* **33:**2094–2099.

Cipolla MJ and Osol G (1998) Vascular smooth muscle actin cytoskeleton in cerebral artery forced dilatation. *Stroke* **29:**1223–1228.

Cipolla MJ, McCall AL, Lessov N, and Porter JM (1997a) Reperfusion decreases myogenic reactivity and alters middle cerebral artery function after focal cerebral ischemia in rats. *Stroke* **28:**176–180.

Cipolla MJ, Porter JM, and Osol G (1997b) High glucose concentrations dilate cerebral arteries and diminish myogenic tone through an endothelial mechanism. *Stroke* **28:**405–410; discussion 410–411.

Cipolla MJ, Lessov N, Hammer ES, and Curry AB (2001) Threshold duration of ischemia for myogenic tone in middle cerebral arteries: effect on vascular smooth muscle actin. *Stroke* **32:**1658–1664.

Clements MK, Siemsen DW, Swain SD, Hanson AJ, Nelson-Overton LK, Rohn TT, and Quinn MT (2003) Inhibition of actin polymerization by peroxynitrite modulates neutrophil functional responses. *J Leukoc Biol* **73:**344–355.

Dailianis S, Patetsini E, and Kaloyianni M (2009) The role of signalling molecules on actin glutathionylation and protein carbonylation induced by cadmium in haemocytes of mussel Mytilus galloprovincialis (Lmk). *J Exp Biol* **212:**3612–3620.
Detre JA, Leigh JS, Williams DS, and Koretsky AP (1992) Perfusion imaging. *Magn Reson Med* **23:**37–45.
Didion SP, Lynch CM, Baumbach GL, and Faraci FM (2005) Impaired endothelium-dependent responses and enhanced influence of Rho-kinase in cerebral arterioles in type II diabetes. *Stroke* **36:**342–347.
Dixon WT, Du LN, Faul DD, Gado M, and Rossnick S (1986) Projection angiograms of blood labeled by adiabatic fast passage. *Magn Reson Med* **3:**454–462.
Dohmen C, Bosche B, Graf R, Reithmeier T, Ernestus RI, Brinker G, Sobesky J, and Heiss WD (2007) Identification and clinical impact of impaired cerebrovascular autoregulation in patients with malignant middle cerebral artery infarction. *Stroke* **38:**56–61.
Drake CT and Iadecola C (2007) The role of neuronal signaling in controlling cerebral blood flow. *Brain Lang* **102:**141–152.
Duckrow RB, Beard DC, and Brennan RW (1987) Regional cerebral blood flow decreases during chronic and acute hyperglycemia. *Stroke* **18:**52–58.
El-Remessy AB, Tawfik HE, Matragoon S, Pillai B, Caldwell RB, and Caldwell RW (2010) Peroxynitrite mediates diabetes-induced endothelial dysfunction: possible role of Rho kinase activation. *Exp Diabetes Res* **2010:**247861.
Elgebaly MM, Portik-Dobos V, Sachidanandam K, Rychly D, Malcom D, Johnson MH, and Ergul A (2007) Differential effects of ET(A) and ET(B) receptor antagonism on oxidative stress in type 2 diabetes. *Vascul Pharmacol* **47:**125–130.
Elgebaly MM, Kelly A, Harris AK, Elewa H, Portik-Dobos V, Ketsawatsomkron P, Marrero M, and Ergul A (2008) Impaired insulin-mediated vasorelaxation in a nonobese model of type 2 diabetes: role of endothelin-1. *Can J Physiol Pharmacol* **86:**358–364.
Elgebaly MM, Prakash R, Li W, Ogbi S, Johnson MH, Mezzetti EM, Fagan SC, and Ergul A (2010) Vascular protection in diabetic stroke: role of matrix metalloprotease-dependent vascular remodeling. *J Cereb Blood Flow Metab* **30:**1928–1938.
Faraci FM and Heistad DD (1990) Regulation of large cerebral arteries and cerebral microvascular pressure. *Circ Res* **66:**8–17.
Fowler M (2008) Microvascular and macrovascular complications of diabetes. *Clin Diabetes* **26:**77–82.
Fukuyama N, Takizawa S, Ishida H, Hoshiai K, Shinohara Y, and Nakazawa H (1998) Peroxynitrite formation in focal cerebral ischemia-reperfusion in rats occurs predominantly in the peri-infarct region. *J Cereb Blood Flow Metab* **18:**123–129.
Girouard H and Iadecola C (2006) Neurovascular coupling in the normal brain and in hypertension, stroke, and Alzheimer disease. *J Appl Physiol* **100:**328–335.
Goto Y, Kakizaki M, and Masaki N (1976) Production of spontaneous diabetic rats by repetition of selective breeding. *Tohoku J Exp Med* **119:**85–90.
Gürsoy-Ozdemir Y, Can A, and Dalkara T (2004) Reperfusion-induced oxidative/nitrative injury to neurovascular unit after focal cerebral ischemia. *Stroke* **35:**1449–1453.
Harris AK, Hutchinson JR, Sachidanandam K, Johnson MH, Dorrance AM, Stepp DW, Fagan SC, and Ergul A (2005) Type 2 diabetes causes remodeling of cerebrovasculature via differential regulation of matrix metalloproteinases and collagen synthesis: role of endothelin-1. *Diabetes* **54:**2638–2644.
Harris AK, Elgebaly MM, Li W, Sachidanandam K, and Ergul A (2008) Effect of chronic endothelin receptor antagonism on cerebrovascular function in type 2 diabetes. *Am J Physiol Regul Integr Comp Physiol* **294:**R1213–R1219.
Hasselbalch SG, Knudsen GM, Capaldo B, Postiglione A, and Paulson OB (2001) Blood-brain barrier transport and brain metabolism of glucose during acute hyperglycemia in humans. *J Clin Endocrinol Metab* **86:**1986–1990.
Humpel C (2011) Chronic mild cerebrovascular dysfunction as a cause for Alzheimer's disease? *Exp Gerontol* **46:**225–232.
Iadecola C (2004) Neurovascular regulation in the normal brain and in Alzheimer's disease. *Nat Rev Neurosci* **5:**347–360.
Jarajapu YP, Guberski DL, Grant MB, and Knot HJ (2008) Myogenic tone and reactivity of cerebral arteries in type II diabetic BBZDR/Wor rat. *Eur J Pharmacol* **579:**298–307.
Jiménez-Altayó F, Caracuel L, Pérez-Asensio FJ, Martínez-Revelles S, Messeguer A, Planas AM, and Vila E (2009) Participation of oxidative stress on rat middle cerebral artery changes induced by focal cerebral ischemia: beneficial effects of 3,4-dihydro-6-hydroxy-7-methoxy-2,2-dimethyl-1(2H)-benzopyran (CR-6). *J Pharmacol Exp Ther* **331:**429–436.
Johansson M and Lundberg M (2007) Glutathionylation of beta-actin via a cysteinyl sulfenic acid intermediary. *BMC Biochem* **8:**26.
Johnson PC (1964) Review of previous studies and current theories of autoregulation. *Circ Res* **15 (Suppl):**2–9.
Kaarisalo MM, Räihä I, Sivenius J, Immonen-Räihä P, Lehtonen A, Sarti C, Mähönen M, Torppa J, Tuomilehto J, and Salomaa V (2005) Diabetes worsens the outcome of acute ischemic stroke. *Diabetes Res Clin Pract* **69:**293–298.
Káplár M, Paragh G, Erdei A, Csongrádi E, Varga E, Garai I, Szabados L, Galuska L, and Varga J (2009) Changes in cerebral blood flow detected by SPECT in type 1 and type 2 diabetic patients. *J Nucl Med* **50:**1993–1998.
Knight RA, Barker PB, Fagan SC, Li Y, Jacobs MA, and Welch KM (1998) Prediction of impending hemorrhagic transformation in ischemic stroke using magnetic resonance imaging in rats. *Stroke* **29:**144–151.
Lecrux C and Hamel E (2011) The neurovascular unit in brain function and disease. *Acta Physiol (Oxf)* **203:**47–59.
Li W, Prakash R, Kelly-Cobbs AI, Ogbi S, Kozak A, El-Remessy AB, Schreihofer DA, Fagan SC, and Ergul A (2010) Adaptive cerebral neovascularization in a model of type 2 diabetes: relevance to focal cerebral ischemia. *Diabetes* **59:**228–235.
Lynch FM, Austin C, Heagerty AM, and Izzard AS (2006) Adenosine- and hypoxia-induced dilation of human coronary resistance arteries: evidence against the involvement of K(ATP) channels. *Br J Pharmacol* **147:**455–458.
Maneen MJ and Cipolla MJ (2007) Peroxynitrite diminishes myogenic tone in cerebral arteries: role of nitrotyrosine and F-actin. *Am J Physiol Heart Circ Physiol* **292:**H1042–H1050.
Maneen MJ, Hannah R, Vitullo L, DeLance N, and Cipolla MJ (2006) Peroxynitrite diminishes myogenic activity and is associated with decreased vascular smooth muscle F-actin in rat posterior cerebral arteries. *Stroke* **37:**894–899.
Mayhan WG (1993) Cerebral circulation during diabetes mellitus. *Pharmacol Ther* **57:**377–391.
Neil HA, Gale EA, Hamilton SJ, Lopez-Espinoza I, Kaura R, and McCarthy ST (1987) Cerebral blood flow increases during insulin-induced hypoglycaemia in type 1 (insulin-dependent) diabetic patients and control subjects. *Diabetologia* **30:**305–309.
Nicolakakis N, Aboulkassim T, Ongali B, Lecrux C, Fernandes P, Rosa-Neto P, Tong XK, and Hamel E (2008) Complete rescue of cerebrovascular function in aged Alzheimer's disease transgenic mice by antioxidants and pioglitazone, a peroxisome proliferator-activated receptor gamma agonist. *J Neurosci* **28:**9287–9296.
Ohara T, Doi Y, Ninomiya T, Hirakawa Y, Hata J, Iwaki T, Kanba S, and Kiyohara Y (2011) Glucose tolerance status and risk of dementia in the community: the Hisayama study. *Neurology* **77:**1126–1134.
Oizumi XS, Akisaki T, Kouta Y, Song XZ, Takata T, Kondoh T, Umetani K, Hirano M, Yamasaki K, Kohmura E, et al. (2006) Impaired response of perforating arteries to hypercapnia in chronic hyperglycemia. *Kobe J Med Sci* **52:**27–35.
Osol G, Laher I, and Cipolla M (1991) Protein kinase C modulates basal myogenic tone in resistance arteries from the cerebral circulation. *Circ Res* **68:**359–367.
Pérez-Asensio FJ, de la Rosa X, Jiménez-Altayó F, Gorina R, Martínez E, Messeguer A, Vila E, Chamorro A, and Planas AM (2010) Antioxidant CR-6 protects against reperfusion injury after a transient episode of focal brain ischemia in rats. *J Cereb Blood Flow Metab* **30:**638–652.
Portik-Dobos V, Harris AK, Song W, Hutchinson J, Johnson MH, Imig JD, Pollock DM, and Ergul A (2006) Endothelin antagonism prevents early EGFR transactivation but not increased matrix metalloproteinase activity in diabetes. *Am J Physiol Regul Integr Comp Physiol* **290:**R435–R441.
Reusch JE (2003) Diabetes, microvascular complications, and cardiovascular complications: what is it about glucose? *J Clin Invest* **112:**986–988.
Schwaninger RM, Sun H, and Mayhan WG (2003) Impaired nitric oxide synthase-dependent dilatation of cerebral arterioles in type II diabetic rats. *Life Sci* **73:**3415–3425.
Sharma SS, Dhar A, and Kaundal RK (2007) FeTPPS protects against global cerebral ischemic-reperfusion injury in gerbils. *Pharmacol Res* **55:**335–342.
Tiago T, Ramos S, Aureliano M, and Gutiérrez-Merino C (2006) Peroxynitrite induces F-actin depolymerization and blockade of myosin ATPase stimulation. *Biochem Biophys Res Commun* **342:**44–49.
Turko IV and Murad F (2002) Protein nitration in cardiovascular diseases. *Pharmacol Rev* **54:**619–634.
Williams DS, Detre JA, Leigh JS, and Koretsky AP (1992) Magnetic resonance imaging of perfusion using spin inversion of arterial water. *Proc Natl Acad Sci USA* **89:**212–216.
Zimmermann PA, Knot HJ, Stevenson AS, and Nelson MT (1997) Increased myogenic tone and diminished responsiveness to ATP-sensitive K+ channel openers in cerebral arteries from diabetic rats. *Circ Res* **81:**996–1004.

Address correspondence to: Dr. Adviye Ergul, Department of Physiology, Georgia Health Sciences University, 1120 15th Street, CA2094, Augusta, GA 30912. E-mail: aergul@georgiahealth.edu